CHEMISTRY
A EUROPEAN JOURNAL

ChemPubSoc
Europe

DOI: 10.1002/chem.201201621

New Chemodosimetric Reagents as Ratiometric Probes for Cysteine and Homocysteine and Possible Detection in Living Cells and in Blood Plasma

Priyadip Das,[a] Amal Kumar Mandal,[a] Nellore Bhanu Chandar,[a] Mithu Baidya,[b] Harshad B. Bhatt,[a] Bishwajit Ganguly,*[a] Sudip K. Ghosh,*[b] and Amitava Das*[a]

Abstract: In this work, we have rationally designed and synthesized two new reagents ($\mathbf{L_1}$ and $\mathbf{L_2}$), each bearing a pendant aldehyde functionality. This aldehyde group can take part in cyclization reactions with β- or γ-amino thiols to yield the corresponding thiazolidine and thiazinane derivatives, respectively. The intramolecular charge-transfer (ICT) bands of these thiazolidine and thiazinane derivatives are distinctly different from those of the molecular probes ($\mathbf{L_1}$ and $\mathbf{L_2}$). Such changes could serve as a potential platform for using $\mathbf{L_1}$ and $\mathbf{L_2}$ as new colorimetric/fluorogenic as well as ratiometric sensors for cysteine (Cys) and homocysteine (Hcy) under physiological conditions. Both reagents proved to be specific towards Cys and Hcy even in the presence of various amino acids, glucose, and DNA. Importantly, these two chemodosimetric reagents could be used for the quantitative detection of Cys present in blood plasma by using a pre-column HPLC technique. Such examples are not common in contemporary literature. MTT assay studies have revealed that these probes have low cytotoxicity. Confocal laser scanning micrographs of cells demonstrated that these probes could penetrate cell membranes and could be used to detect intracellular Cys/Hcy present within living cells. Thus, the results presented in this article not only demonstrate the efficiency and specificity of two ratiometric chemodosimeter molecules for the quantitative detection of Cys and Hcy, but also provide a strategy for developing reagents for analysis of these vital amino acids in biological samples.

Keywords: charge transfer · chemodosimetric detection · cysteine/homocysteine sensors · fluorescent probes · imaging agents · ratiometric probes

Introduction

Among low molecular weight thiols, important amino acids such as cysteine (Cys) and homocysteine (Hcy) play crucial roles in physiological matrices due to their participation in critical redox processes and cellular growth.[1,2] Cys and Hcy are produced intracellularly during the metabolism of methionine.[3] These are important constituents of the protective antioxidant systems of the body. A deficiency of Cys leads to diseases such as hematopoiesis decrease, leukocyte loss, psoriasis, slowed growth, liver damage, skin lesions, hair depigmentation, edema, and so on.[4] Elevated levels of Hcy have been recognized as an independent risk factor for cardiovascular disease.[5] This is also associated with various diseases or clinical conditions, which include Alzheimer's disease, schizophrenia, end-stage renal disease, osteoporosis, and type II diabetes.[6] Although Hcy has been associated with several diseases, the mechanisms underlying its deleterious influences have not yet been completely elucidated.[7] These findings have necessitated the development of suitable reagents that may be used not only for selective and efficient detection of these two critical thio-amino acids under physiological conditions, but also for fluorescence bioimaging analyses for in vivo detection. These aims are of direct relevance to diagnostic applications and investigating the functions of these two amino acids in cells. Methods for the direct detection of Cys/Hcy are usually hampered by interference from structurally related molecules such as glutathione (GSH). A number of analytical methods for the detection of Cys and Hcy have been developed using high-performance liquid chromatography (HPLC),[8] capillary electrophoresis,[9] electrochemical assay,[10] UV/Vis spectroscopy,[11] FTIR spectroscopy,[12] mass spectrometry,[13] and fluorescence spectroscopy.[14] Among these, methods based on electronic and fluorescence spectral responses are more appealing due to the simplicity of the measurement processes, high sensitivity, and reliability.[15] Furthermore, fluorescence-based probe molecules offer the possibility of bioimaging applications in living cells with temporal and spatial

[a] P. Das, A. K. Mandal, N. B. Chandar, H. B. Bhatt, B. Ganguly, Dr. A. Das
CSIR-Central Salt and Marine Chemicals Research Institute
Bhavnagar, 364002, Gujarat (India)
Fax: (+91) 278-256-7562
E-mail: ganguly@csmcri.org
amitava@csmcri.org

[b] M. Baidya, Dr. S. K. Ghosh
Department of Biotechnology
Indian Institute of Technology
Kharagpur West Bengal-721302 (India)
E-mail: sudip@hijli.iitkgp.ernet.in

Supporting information for this article is available on the WWW under http://dx.doi.org/10.1002/chem.201201621.

resolution.[14c,i,16] Despite such advantages, examples of colorimetric and/or fluorescent dual ratiometric probes for optical detection of Hcy and Cys remain rare.[14c,17] Most reported reagents for the optical detection of these two amino acids have been based on the chemodosimetric approach,[15b,d,16a,17a,18] whereby cyclization reactions of β-/γ-amino alkyl thiols (containing both -SH and -NH_2 groups) with organic aldehydes generate the respective thiazolidine and thiazinane derivatives. In general, thiazolidine and thiazinane derivatives have distinctly different ICT processes as compared to the reactant aldehyde components, and this results in either an on-off or a ratiometric optical response, with the sole exception of one example in which a photoinduced electron-transfer (PET) process gives rise to a fluorescence on-off response.[18] The majority of such molecular probes for Cys or Hcy are either based on colorimetric changes for visual detection or on fluorescence turn off-on responses.

In this regard, ratiometric fluorescent probes are even more significant as they allow simultaneous detection at two different wavelengths and have a built-in correction for variation in sample environment and probe distribution. More importantly, studies on the possibility of using such reagents as diagnostic probe molecules for quantitative detection of these two amino acids in blood plasma have been extremely rare in the literature.[11b,d,19]

In this article, we report two new reagents ($\mathbf{L_1}$ and $\mathbf{L_2}$; Scheme 1) for the ratiometric detection of Cys and Hcy under physiological conditions following the chemodosimetric approach, both of which serve as dual-channel (electronic and fluorescence spectra) ratiometric probes. We have rationalized the bathochromic and hypsochromic shifts in the ICT bands of $\mathbf{L_1}$ and $\mathbf{L_2}$ upon reaction with Cys or Hcy by performing quantum chemical calculations. Both of these reagents have proved to be specific for Cys or Hcy, even in the presence of other amino acids, glucose, DNA, and related thio-containing compounds such as GSH or 2-mercaptoethanol (MER). Both reagents could be used for the quantitative detection of Cys present in blood serum as well as for in vivo fluorescence imaging in the detection of intracellular Cys/Hcy in living HeLa cells, which may have special significance in medicinal biology and diagnostic applications.

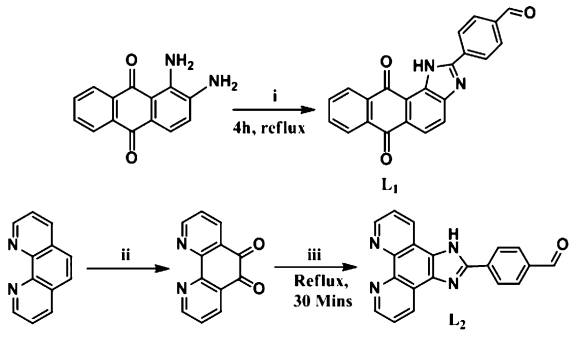

(i) terephthalaldehyde, EtOH, CF_3CO_2H; (ii) Conc H_2SO_4 +Conc HNO_3 (2:1), KBr; (iii) terephthalaldehyde, NH_4OAc, CH_3CO_2H,

Scheme 1. Methodologies adopted for the synthesis of $\mathbf{L_1}$ and $\mathbf{L_2}$.

Results and Discussion

Synthesis: Receptor $\mathbf{L_1}$ was synthesized in one step in a reasonably good yield by a condensation reaction of 1,2-diamino anthraquinone with terephthalaldehyde. Similarly, $\mathbf{L_2}$ was obtained by refluxing a mixture of 1,10-phenanthroline-5,6-dione and terephthalaldehyde in acetic acid in the presence of ammonium acetate. Both reagents were characterized by standard analytical and spectroscopic techniques, and all analytical data were in good agreement with the proposed formulations as well as the desired purities.

Absorption and emission spectral properties of $\mathbf{L_1}$ and $\mathbf{L_2}$: Absorption and photoluminescence spectra of $\mathbf{L_1}$ and $\mathbf{L_2}$ were recorded at room temperature (Figure 1). The longer wavelength absorption band maximum for $\mathbf{L_1}$ at 397 nm ($\varepsilon = 1.92\times10^3\ dm^3\,mol^{-1}\,cm^{-1}$) may be attributed primarily to a spin-allowed intramolecular charge transfer (ICT) ($\pi_{imidazole}$–$\pi^*_{anthraquinone}$) band, while for $\mathbf{L_2}$ the corresponding band at 346 nm ($\varepsilon = 1.2\times10^4\ dm^3\,mol^{-1}\,cm^{-1}$) may also be ascribed to an ICT-based process (π_{phen}–$\pi^*_{imidazole\ aldehyde}$). The ICT nature of these absorption bands was further confirmed by

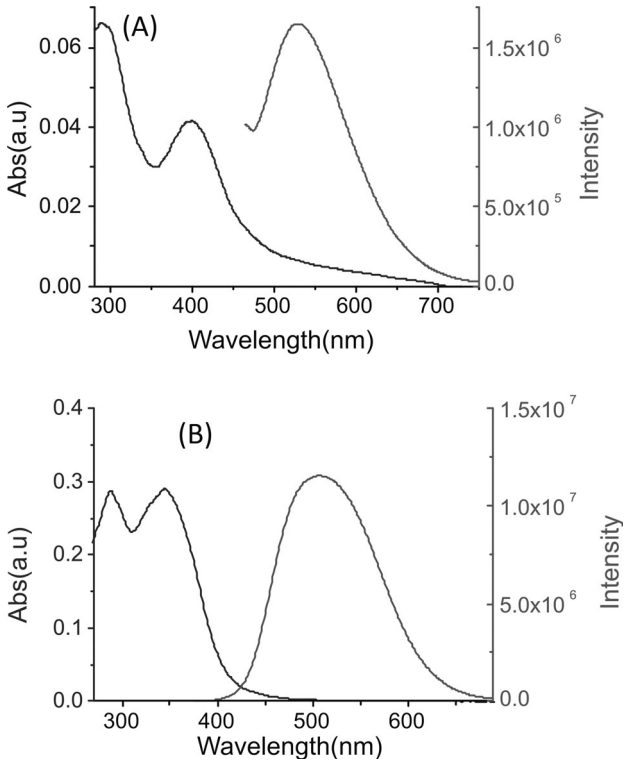

Figure 1. (A) Absorption and emission spectra of $\mathbf{L_1}$ (2.0×10^{-5} M) in DMSO/aqueous HEPES buffer (3:2, *v*/*v*, pH 7.4) medium and (B) absorption and emission spectra of $\mathbf{L_2}$ (2.0×10^{-5} M) in DMSO/aqueous HEPES buffer (8:2, *v*/*v*, pH 7.4) medium at 25 °C. For the emission spectra, λ_{ext} of 397 nm was used for $\mathbf{L_1}$, while that for $\mathbf{L_2}$ was 346 nm.

their red shifts with increasing solvent polarity (see Figures S13 and S15 in the Supporting Information). $\mathbf{L_1}$ and $\mathbf{L_2}$ show strong ICT emission peaks at 528 nm (λ_{ext} of 397 nm) and 506 nm (λ_{ext} of 346 nm), respectively. The relative luminescence quantum yields for $\mathbf{L_1}$ (Φ_{L1}) and $\mathbf{L_2}$ (Φ_{L2}) in air-equilibrated DMSO/aqueous HEPES buffer (3:2, *v*/*v*, pH 7.4 for $\mathbf{L_1}$ and 4:1, *v*/*v*, pH 7.4 for $\mathbf{L_2}$) were evaluated as $\Phi_{L1}=0.0066$ and $\Phi_{L2}=0.45$ by using Equation (1) with quinine sulfate as a standard.

Optical responses: It is known that an aldehyde moiety can undergo a selective cyclization reaction with β-/γ-amino alkyl thiols to yield the corresponding thiazolidines and this was the primary reason that led to the design of receptor molecules $\mathbf{L_1}$ and $\mathbf{L_2}$ with pendant aldehyde functionalities.[20] The formation of the respective thiazolidine derivatives upon reaction with $\mathbf{L_1}$ or $\mathbf{L_2}$ was expected to perturb the energies of the frontier molecular orbitals (FMO) and hence the associated energy gaps for the ICT-based processes, which would otherwise remain operational for the individual receptor molecules.

UV/Vis responses: The recognition of Cys/Hcy by $\mathbf{L_1}$ and $\mathbf{L_2}$ was investigated by monitoring the changes in the electronic spectra of these receptors upon the formation of their respective thiazolidine moieties. Thus, $\mathbf{L_1}$ and $\mathbf{L_2}$ were each treated with varying concentrations of Cys and Hcy in appropriate DMSO/aqueous HEPES buffer (pH 7.4) media. Upon addition of increasing amounts of Cys or Hcy to a solution of $\mathbf{L_1}$ in DMSO/aqueous HEPES buffer (50 mM, 3:2 (*v*/*v*), pH 7.4), the absorption band at around 397 nm was found to decrease gradually with a concomitant increase at around 460 nm. Eventually, the band with a maximum at 397 nm disappeared and a new red-shifted ($\Delta\lambda\approx65$ nm) absorption band with a maximum at 464 nm (for Cys) or 462 nm (for Hcy) appeared, along with two distinct isosbestic points at 367 and 409 nm (Figure 2). Both isosbestic points appeared simultaneously, which suggested the presence of only two absorbing species in equilibrium. These changes were associated with a visually detectable change in solution colour from yellow to orange (Figure 2(C)) and revealed the possibility of using this reagent as a sensitive colorimetric reagent for the visual detection of Cys and Hcy. For the other receptor $\mathbf{L_2}$ in DMSO/aqueous HEPES buffer (50 mM, 8:2 (*v*/*v*), pH 7.4), a similar experiment resulted a new blue-shifted ($\Delta\lambda\approx70$ nm) band maximum at around 276 nm, while the original spectral band of $\mathbf{L_2}$ with a maximum at 346 nm disappeared. These spectral changes were associated with the appearance of a new isosbestic point at around 336 nm (Figure 3) and signified the presence of two equilibrating components. It may be noted that for $\mathbf{L_2}$ the spectral changes were restricted to the UV region and thus no associated colour change could be detected visually.

Emission responses: Formation of the thiazolidine/thiazinane derivatives by reactions of $\mathbf{L_1}$ and $\mathbf{L_2}$ with Cys and Hcy were also investigated by photoluminescence spectroscopy (Figures 4 and 5). An appreciable red-shift in the emission band maximum of $\mathbf{L_1}$ from 528 nm to 598 nm ($\lambda_{ext}=397$ nm) associated with a visually detectable change in solution fluorescence from yellow to red was observed.

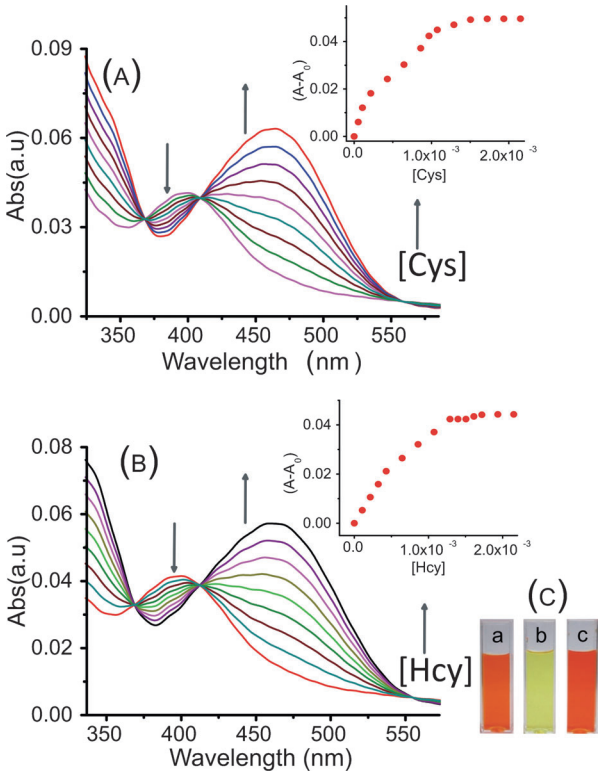

Figure 2. Changes in the UV/Vis spectra of $\mathbf{L_1}$ (2.15×10^{-5} M) in DMSO/aqueous HEPES buffer (50 mM, 3:2 (*v*/*v*); pH 7.4) medium with varying concentrations of (A) Cys ($0–2.15\times10^{-3}$ M) and (B) Hcy ($0–2.58\times10^{-3}$ M) at 25 °C. Insets: titration curves of $\mathbf{L_1}$ with varying [Cys] (0–100 mole equiv) and [Hcy] (0–100 mole equiv). (C) Photographs showing the change of the solution colour of $\mathbf{L_1}$ in the absence (b) and presence of (a) Cys and (c) Hcy.

For Cys, two isosbestic points appeared simultaneously at 492 and 577 nm, while for Hcy two isosbestic points appeared at 495 and 577 nm. For $\mathbf{L_2}$, however, upon addition of increasing amounts of Cys or Hcy, a new blue-shifted emission band appeared at around 438 nm ($\lambda_{ext}=346$ nm), with a concomitant decrease in the emission intensity at 506 nm, the emission band maximum associated with the ICT transition for $\mathbf{L_2}$. An isosbestic point appeared at 457 nm, with an associated visual change in the solution fluorescence from green to blue (Figure 5). The observed shifts in the emission band maxima for $\mathbf{L_1}$ and $\mathbf{L_2}$ upon formation of the thiazolidine/thiazinane derivatives were in good agreement with the results of the absorption spectral studies. In order to understand the exact nature of the electronic transitions associated with these thiazolidine or thiazinane derivatives, theoretical calculations were performed. Understandably, the electron-withdrawing influence of the pendant aldehyde functionality also played a crucial role in the modification of this photoinduced signal transduction process.

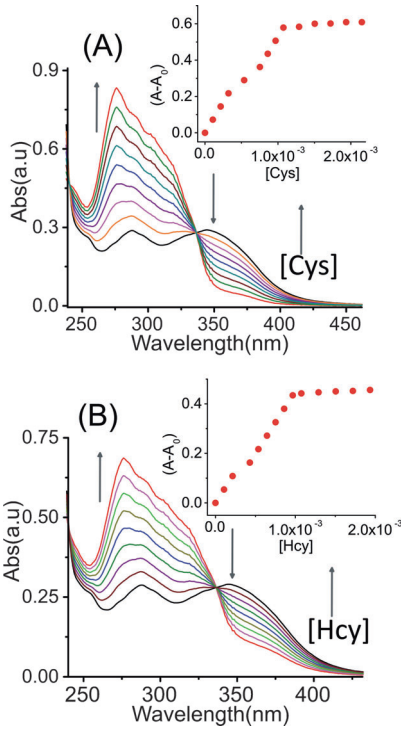

Figure 3. Changes in the UV/Vis spectra of $\mathbf{L_2}$ (2.0×10^{-5} M) in DMSO/aqueous HEPES buffer (50 mM, 8:2 (v/v); pH 7.4) medium with varying concentrations of (A) Cys (0–2.0×10^{-3} M) and (B) Hcy (0–2.40×10^{-3} M) at 25 °C. Insets: titration curves of $\mathbf{L_2}$ with varying [Cys] (0–100 mole equiv) and [Hcy] (0–100 mole equiv).

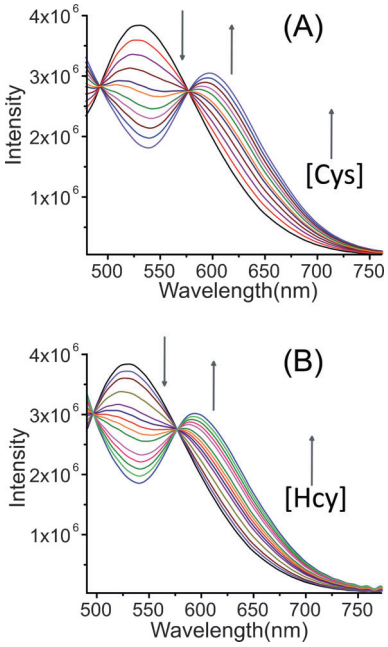

Figure 4. Systematic changes in the fluorescence spectral pattern for $\mathbf{L_1}$ (2.15×10^{-5} M) in DMSO/aqueous HEPES buffer (50 mM, 3:2 (v/v); pH 7.4) medium upon addition of increasing concentrations of (A) Cys (0–2.15×10^{-3} M) and (B) Hcy (0–2.58×10^{-3} M) at 25 °C; a λ_{ext} of 397 nm was used for all of these studies.

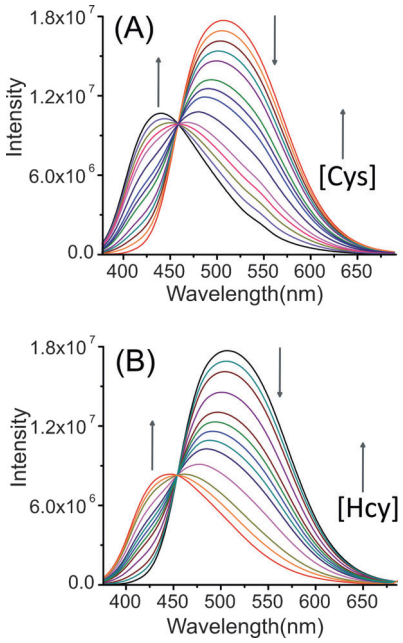

Figure 5. Systematic changes in the fluorescence spectral pattern for $\mathbf{L_2}$ (2.0×10^{-5} M) in DMSO/aqueous HEPES buffer (50 mM, 8:2 (v/v), pH 7.4) medium upon addition of increasing concentrations of (A) Cys (0–2.0×10^{-3} M) and (B) Hcy (0–2.40×10^{-3} M) at 25 °C; a λ_{ext} of 346 nm was used.

DFT calculations: In order to understand the nature of the transitions responsible for the observed spectral bands for $\mathbf{L_1}$/$\mathbf{L_2}$ and their corresponding thiazolidine/thiazinane derivatives, DFT calculations were performed to optimize the geometries of the respective species (Figure 6) at the B3LYP/6-31G(d) level of theory. Single-point calculations were performed at the B3LYP/6-311+G(2d,p) level using the B3LYP/6-31G(d)-optimized geometries for more accurate estimation of the energies. The frontier molecular orbitals (FMO) and their energy differences are also shown in Figure 6. The FMO analyses revealed that for $\mathbf{L_1}$, $\mathbf{L_1}$-Cys, and $\mathbf{L_1}$-Hcy the orbital coefficients of the HOMOs are mainly located on the imidazole and phenyl moieties, while the coefficients of the LUMOs are distributed over the anthraquinone moieties (Figure 6). The computed frontier orbital energy differences revealed that the energy gap was narrowed on going from parent $\mathbf{L_1}$ to its derivatives $\mathbf{L_1}$-Cys and $\mathbf{L_1}$-Hcy. The calculated energy gaps for $\mathbf{L_1}$, $\mathbf{L_1}$-Cys, and $\mathbf{L_1}$-Hcy are 3.3, 3.1, and 3.2 eV, respectively (Figure 6). These results are in good qualitative agreement with the observed red-shifts in the absorption and emission spectra of $\mathbf{L_1}$ and its corresponding $\mathbf{L_1}$-Cys and $\mathbf{L_1}$-Hcy derivatives. Thus, for $\mathbf{L_1}$ and its derivatives, the charge-transfer transitions predominantly involve imidazole donor and anthraquinone acceptor moieties. In the case of $\mathbf{L_2}$ and its derivatives ($\mathbf{L_2}$-Cys and $\mathbf{L_2}$-Hcy), the orbital coefficients were found to be largely located on the 1,10-phenanthroline moieties for the HOMOs (Figure 6), while the orbital coefficients for the LUMOs were partially located on the imidazole moieties. Interestingly, the computed FMO energy differences revealed that the HOMO–LUMO energy gaps were enhanced

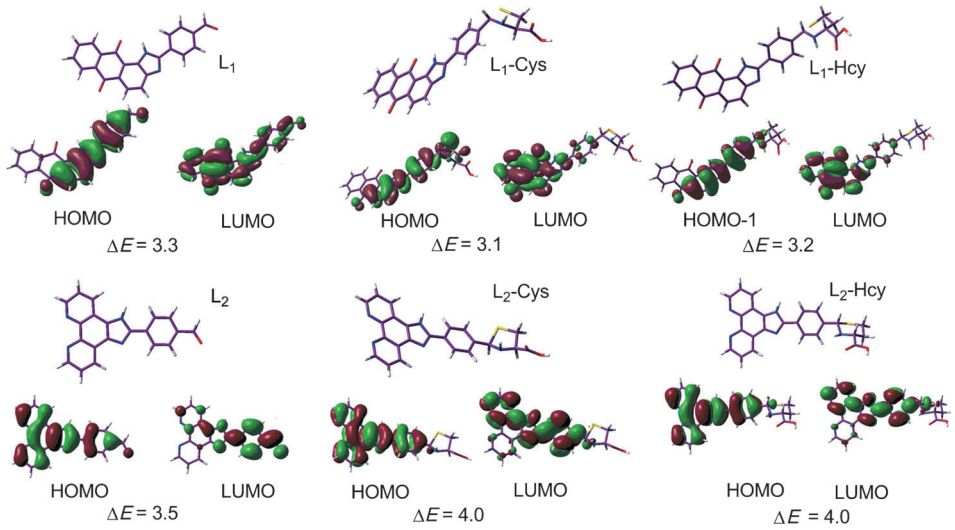

Figure 6. Optimized geometries of $\mathbf{L_1}$ and $\mathbf{L_2}$ and their respective thiazolidine and thiazinane derivatives at the B3LYP/6-31G(d) level of theory. Frontier molecular orbitals of $\mathbf{L_1}$, $\mathbf{L_1}$-Cys, $\mathbf{L_1}$-Hcy and $\mathbf{L_2}$, $\mathbf{L_2}$-Cys, $\mathbf{L_2}$-Hcy calculated at the B3LYP/6-31G(d) level of theory. Energy gaps (ΔE) between HOMOs and LUMOs were calculated at the B3LYP/6-311+G(2d,p)//B3LYP/6-31G(d) level of theory (eV).

on going from parent $\mathbf{L_2}$ to its derivatives $\mathbf{L_2}$-Cys and $\mathbf{L_2}$-Hcy (Figure 6), which is consistent with the observed blue shifts in the absorption and luminescence spectra of these systems. However, excitation spectra recorded for $\mathbf{L_2}$-Cys (with $\lambda_{ems}=438$ nm) in DMSO (Figure S17 in the Supporting Information) suggested that besides these charge-transfer transitions, a transition associated with a 1,10-phenanthroline-based excited state also contributed to the observed emission band at 434 nm for $\mathbf{L_2}$-Cys.

TCSPC studies: The ratiometric luminescence responses of the receptors $\mathbf{L_1}$ and $\mathbf{L_2}$ in the presence of Cys were also confirmed by the results of time-correlated single-photon counting (TCSPC) studies. Time-resolved emission decay studies on $\mathbf{L_1}$, $\mathbf{L_2}$, $\mathbf{L_1}$-Cys, and $\mathbf{L_2}$-Cys were carried out using either a 405 nm laser or a 360 nm LED as the excitation source. Details of the lifetime components of the excited states of $\mathbf{L_1}$, $\mathbf{L_2}$, $\mathbf{L_1}$-Cys, and $\mathbf{L_2}$-Cys at their respective emission maxima as well as their isoemissive points (Figures 4 and 5) are summarized in Table 1. Comparison of the decay components and their relative contributions (Table 1) for $\mathbf{L_1}$/$\mathbf{L_2}$ with those for $\mathbf{L_1}$-Cys/$\mathbf{L_2}$-Cys at three different monitoring wavelengths clearly reveals the ratiometric emission responses upon formation of $\mathbf{L_1}$-Cys and $\mathbf{L_2}$-Cys from the respective probe reagents $\mathbf{L_1}$ and $\mathbf{L_2}$. It is not unreasonable to presume that a similar trend will be followed for $\mathbf{L_1}$-Hcy and $\mathbf{L_2}$-Hcy formation.

Chemodosimetric detection of Cys and Hcy: Conversion of the electron-withdrawing aldehyde group to the corresponding thiazolidine or thiazinane derivative upon reaction with Cys or Hcy, respectively, resulted in a significant change in the nature of the CT process and led to a distinct change in the spectral pattern. This facilitated visual detection of Cys or Hcy in DMSO/aqueous HEPES buffer medium. Associated changes in the emission spectral patterns were significant, and this also allowed visual detection of these two crucial amino acids in physiological environments. It was evident from the FMOs (Figure 6) that the LUMOs for $\mathbf{L_1}$ or $\mathbf{L_2}$ were partially distributed over the respective aldehyde functionalities, and the absence of such influence in the corresponding thiazolidine or thiazinane moieties contributed to the observed changes in the absorption and emission spectral patterns. As mentioned above, changes in the absorption spectrum of $\mathbf{L_2}$ are limited to the UV region and thus cannot be detected visually. Importantly, a Stokes shift of about 200 nm could be achieved when $\mathbf{L_1}$ was used as a chemodosimetric reagent, while the shift for $\mathbf{L_2}$ was approximately 96 nm (Scheme 2). These results opened up the possibility of the ratiometric detection of these two important amino acids under physiological conditions at pH 7.4. To investigate the utility of $\mathbf{L_1}$ and $\mathbf{L_2}$ as ratiometric luminescent probes for the quantitative detection of Cys/Hcy, their emission intensities in the presence of varying concentrations of Cys or Hcy were measured in appropriate DMSO/aqueous HEPES buffer media at room temperature. It is evident from Figure 4 that with a gradual increase in [Cys] or [Hcy], the emission intensity from the solution of $\mathbf{L_1}$ at 528 nm (I_{528}) decreased gradually with a concomitant increase in the emission intensity at about 598 nm (I_{598}). The plots of I_{598}/I_{528} versus [Cys] or [Hcy] were found to be linear and showed significant changes in the ratio (I_{598}/I_{528}) from 0.52 to 1.61 for Cys and from 0.56 to 1.53 for Hcy (Figure 7(A, B)). Similarly, for $\mathbf{L_2}$, the I_{506} was found to decrease with a concomitant increase in I_{438} with increasing [Cys]

Table 1. Time-resolved emission decay constants for $\mathbf{L_1}$, $\mathbf{L_2}$, $\mathbf{L_1}$-Cys, $\mathbf{L_2}$-Cys, and analogous components in appropriate DMSO/aqueous HEPES buffer (pH 7.4) medium at 295 K using either a 405 nm laser pulse or a 360 nm LED as excitation source.

Compound	λ_{ext} [nm]	λ_{mon} [nm]	Time constant [ns]	χ^2
$\mathbf{L_1}$	405	528[a]	$\tau_1=0.16$ (76.61 %)[d] $\tau_2=4.17$ (23.39 %)[e]	1.001
$\mathbf{L_1}$-Cys	405	577[b]	$\tau_1=0.12$ (35 %)[d] $\tau_2=3.83$ (65 %)[e]	1.21
$\mathbf{L_1}$-Cys	405	598[c]	$\tau_1=0.11$ (25.58 %)[d] $\tau_2=3.86$ (74.42 %)[e]	1.22
$\mathbf{L_2}$	360	506[a]	$\tau_1=2.43$ (100 %)[f]	1.08
$\mathbf{L_2}$-Cys	360	459[b]	$\tau_1=1.86$ (16 %)[f] $\tau_2=4.86$ (84 %)[g]	1.16
$\mathbf{L_2}$-Cys	360	436[c]	$\tau_1=5.244$ (100 %)[g]	1.07

[a] Monitored at emission maxima of $\mathbf{L_1}$ or $\mathbf{L_2}$. [b] Measured at isoemissive point of the emission spectra. [c] Monitored at emission maxima of $\mathbf{L_1}$-Cys or $\mathbf{L_2}$-Cys. [d] Anthraquinone-based CT process. [e] Predominantly modified imidazole to anthraquinone-based CT process. [f] Predominantly modified imidazole to Phen-based CT process. [g] Phen-based emission process.

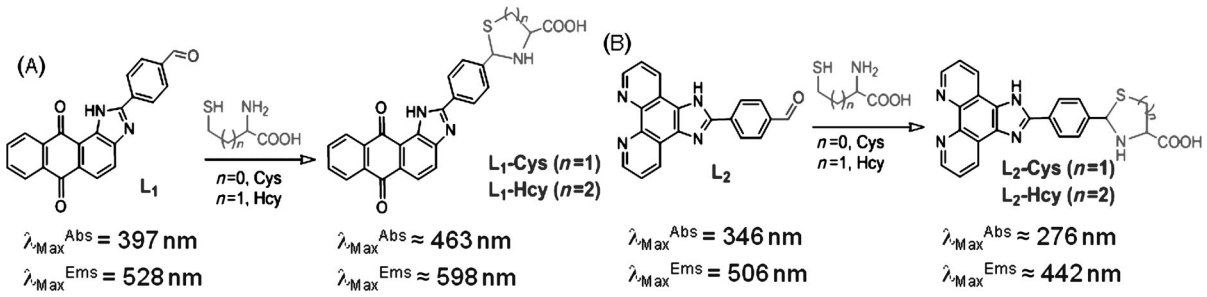

Scheme 2. Schematic representation of the chemodosimetric detection of Cys and Hcy using (A) $\mathbf{L_1}$ and (B) $\mathbf{L_2}$ as probe reagent in DMSO/aqueous HEPES buffer medium of pH 7.4.

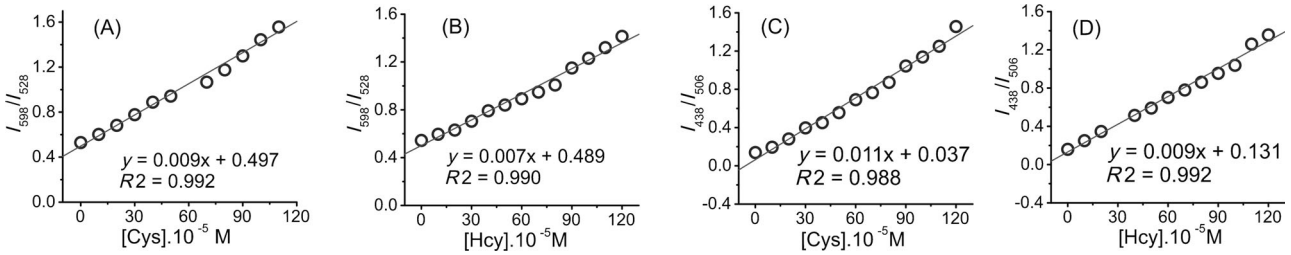

Figure 7. Plots of luminescence intensity ratio of $\mathbf{L_1}$ at 598 nm to 528 nm as a function of various concentrations of (A) Cys and (B) Hcy in a DMSO/aqueous HEPES buffer (pH 7.4; $v/v = 3{:}2$) medium; similar plots I_{438}/I_{506} vs. [X]; X being (C) Cys or (D) Hcy for $\mathbf{L_2}$ in a DMSO/aqueous HEPES buffer (pH 7.4, $v/v = 8{:}2$) medium.

or [Hcy], and significant increases in the ratio I_{438}/I_{506} from 0.13 to 2.06 for Cys and from 0.16 to 1.65 for Hcy were achieved (Figure 7(C, D)). The above results clearly demonstrate that these two new molecules ($\mathbf{L_1}$ and $\mathbf{L_2}$) could be used as ratiometric as well as a chemodosimetric fluorescent probes for selective and quantitative detection of Cys and Hcy. Time-dependent fluorescence spectra of $\mathbf{L_1}$ and $\mathbf{L_2}$ in the presence of Cys or Hcy (50 mole equiv) were measured in appropriate solvent mixtures (see Figures S18–S21 in the Supporting Information). The results of these studies indicated that the reactions were essentially complete after about 55 min, a reaction time comparable to those reported for chemodosimetric detection of these two amino acids.[11d,17a,21] Therefore, an assay time of about 55 min was chosen in the evaluation of the selectivity and sensitivity of these receptors towards Cys and Hcy.

^{1}H NMR studies: The interactions of $\mathbf{L_1}$ and $\mathbf{L_2}$ with Cys were also investigated by ^{1}H NMR spectroscopy in [D_6]DMSO solution, and the results are shown in Figure 8. In the presence of excess of Cys (100 mole equiv), the signal corresponding to the aldehyde protons (-CHO) at $\delta \approx 10$ ppm for $\mathbf{L_1}$ or $\mathbf{L_2}$ disappeared. Two new signals appeared at $\delta \approx 6$ ppm and $\delta \approx 13$–14 ppm, which could be assigned to the methine proton and carboxylic hydrogen (-COOH), respectively, of the thiazolidine product.[11b–e,16a] In the absence of the strong electron-withdrawing effect of the -CHO functionality in the thiazolidine derivative, the resonances of the protons of the phenyl ring were shifted upfield.

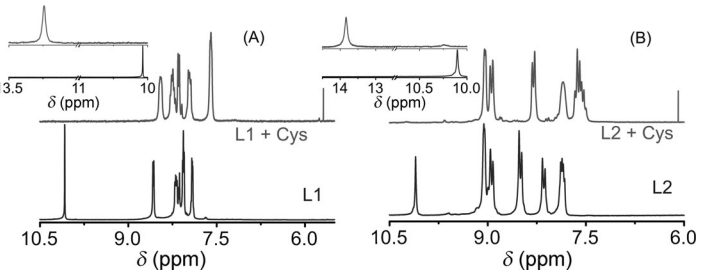

Figure 8. ^{1}H NMR spectra of (A) $\mathbf{L_1}$, $\mathbf{L_1}$-Cys and (B) $\mathbf{L_2}$, $\mathbf{L_2}$-Cys in [D_6]DMSO solution. The signals at $\delta \approx 10$ ppm are assigned to the aldehyde protons of $\mathbf{L_1}$ and $\mathbf{L_2}$. Signals at $\delta \approx 6$ ppm and $\delta \approx 14$ ppm (insets) are assigned to the methine and carboxylic protons, respectively.

Mass spectrometry and FTIR analysis: In order to confirm the formation of the thiazolidine derivatives ($\mathbf{L_1}$-Cys, $\mathbf{L_2}$-Cys), $\mathbf{L_1}$ and $\mathbf{L_2}$ were treated with Cys and the reaction products were isolated and characterized by mass spectrometry and FTIR spectroscopy. The isolated reaction products were found to have identical molecular ion peaks (Figures S22 and S23 in the Supporting Information) as well as similar absorption/emission spectra when compared with those observed for the respective thiazolidine derivatives $\mathbf{L_1}$-Cys and $\mathbf{L_2}$-Cys obtained in solution by reaction of $\mathbf{L_1}$ or $\mathbf{L_2}$ with Cys (Figures S29 and S30 in the Supporting Information). The corresponding spectra for Hcy derivatives could not be measured due to the limited solubility of Hcy in common organic solvents. The FTIR spectra of the receptors showed sharp bands at $\tilde{\nu} = 1670\ \mathrm{cm^{-1}}$ for $\mathbf{L_1}$ and $1693\ \mathrm{cm^{-1}}$ for $\mathbf{L_2}$, characteristic of an aromatic C=O functionality. The

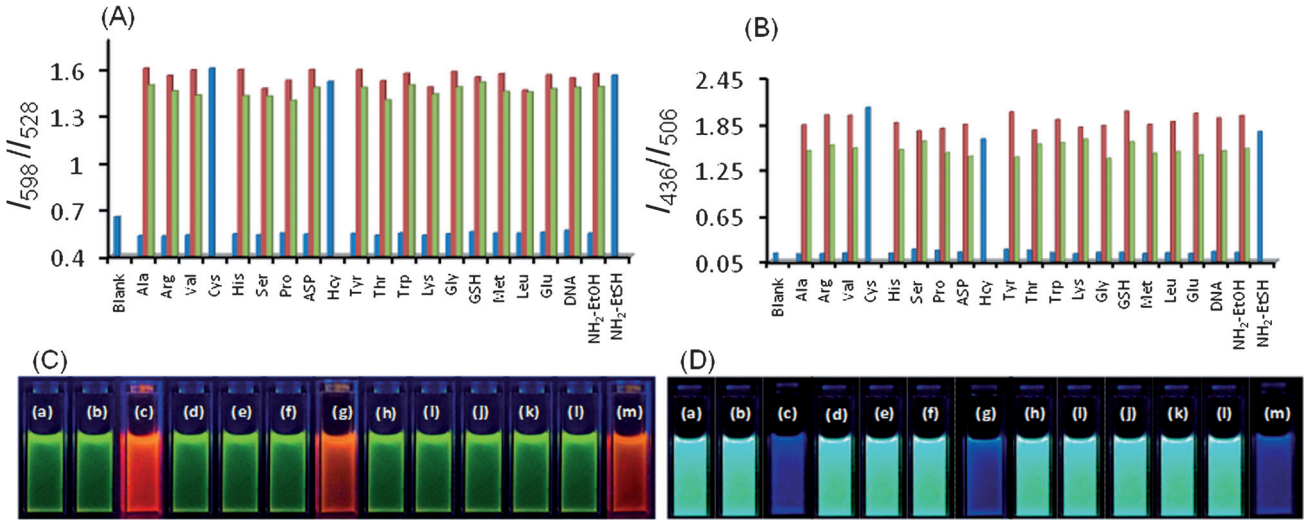

Figure 9. Luminescence intensity ratios (A) I_{598}/I_{528} for $\mathbf{L_1}$ (20 μM) and (B) I_{438}/I_{506} for $\mathbf{L_2}$ (20 μM) in the presence of different amino acids, glucose, CT-DNA, ethanolamine, and cysteamine (1 mM; the blue bars). The red and green bars show the respective luminescence intensity ratios of $\mathbf{L_1}$ and $\mathbf{L_2}$ (20 μM) with different amino acids, glucose, CT-DNA, and ethanolamine (1 mM) in the presence of Cys (1 mM; red bars) and Hcy (1 mM; green bars). Photographs showing the luminescence of (C) $\mathbf{L_1}$ (left) and (D) $\mathbf{L_2}$ (right) in the presence of different molecules (a, blank; b, Gly; c, Cys; d, Ala; e, GSH; f, Arg; g, Hcy; h, Lys; i, Ser; j, glucose; k, CT-DNA; l, ethanolamine; m, cysteamine, when illuminated with a 365 nm UV lamp.

absence of these characteristic signals from the FTIR spectra of the isolated $\mathbf{L_1}$-Cys and $\mathbf{L_2}$-Cys confirmed the conversion of the aldehyde functionalities into the respective thiazolidine derivatives upon reaction with Cys (see Figure S26 in the Supporting Information).

Reactions of $\mathbf{L_1}$ and $\mathbf{L_2}$ with different amino acids, cystine, glucose, DNA, and hydroxy/mercapto ethylamines, and their selective optical responses: In general, a problem associated with most literature procedures for the direct detection of Cys/Hcy is interference in the detection process by structurally related molecules, such as thiol-bearing peptides, glutathione (GSH), other amino acids, 2-mercaptoethanol, and hydroxy/mercapto ethylamines.[14l,15c,16e] In order to evaluate the recognition specificity of the two chemodosimetric reagents $\mathbf{L_1}$ and $\mathbf{L_2}$ towards Cys/Hcy, we extended our studies to other amino acids, cystine, glucose, CT-DNA, ethanolamine ($NH_2CH_2CH_2OH$), cysteamine ($NH_2CH_2CH_2SH$), and 2-mercaptoethanol ($SHCH_2CH_2OH$) in an appropriate DMSO/aqueous HEPES buffer medium of pH 7.4 at room temperature.

Neither $\mathbf{L_1}$ (20 μM) nor $\mathbf{L_2}$ (20 μM) showed any significant changes in their absorption and emission spectral patterns (Figures S9–S12 in the Supporting Information) upon addition of excesses (1 mM) of various amino acids, such as glycine (Gly), leucine (Leu), aspartic acid (Asp), proline (Pro), arginine (Arg), lysine (Lys), valine (Val), glutathione (GSH), alanine (Ala), threonine (Thr), histidine (His), tryptophan (Trp), tyrosine (Tyr), serine (Ser), or methionine (Met), cystine, CT-DNA, $NH_2CH_2CH_2OH$, or 2-mercaptoethanol. Spectral changes were only observed for $\mathbf{L_1}$ or $\mathbf{L_2}$ when a solution of one of the β-/γ-aminoalkyl thiols, such as Cys, Hcy, or $NH_2CH_2CH_2SH$ was added, which signifies formation of the corresponding thiazolidine or thiazinane derivative. Furthermore, to evaluate the utility of $\mathbf{L_1}$ and $\mathbf{L_2}$ as chemodosimetric probes for the detection of Cys/Hcy in complex biological fluids or samples, competitive studies were also performed by monitoring the emission intensities of $\mathbf{L}_x$-Cys or $\mathbf{L}_x$-Hcy ($x = 1$ or 2) in the presence of a large excess (50 mole equivalents) of different amino acids, glucose, CT-DNA, or ethanolamine (Figure 9(A, B)). No significant changes in the emission spectral properties of $\mathbf{L}_x$-Cys or $\mathbf{L}_x$-Hcy were observed. This confirmed that none of these amino acids, nor glucose, CT-DNA, or ethanolamine, had any influence on the detection of Cys or Hcy by $\mathbf{L_1}$ or $\mathbf{L_2}$. Figure 9(C, D) further reveal that the emission colour variation of $\mathbf{L_1}$ and $\mathbf{L_2}$ upon formation of the corresponding thiazolidine and thiazinane derivatives could be detected visually.

Cytotoxicity: The cytotoxicities of $\mathbf{L_1}$ and $\mathbf{L_2}$ towards cervical cancer (HeLa) cells were evaluated by means of MTT assays. Cell proliferation was checked after 12 h following a standard protocol (see the Supporting Information). No remarkable differences in the proliferation of the cells were observed in the absence or presence of 1–25 μM of $\mathbf{L_1}$ or $\mathbf{L_2}$ (Figure 10). The cellular viability was estimated to be 80% after incubation for 12 h at $[\mathbf{L_1}]$ or $[\mathbf{L_2}]$ $\leq$25 μM. Considering the reaction time of 55 min, it is concluded that the cytotoxicities of $\mathbf{L_1}$ and $\mathbf{L_2}$ ($\leq$25 μM) are likely to be very low.

Cell imaging and possible detection of intercellular Cys and Hcy: The suitable amphipathicity and insignificant cytotoxicity of $\mathbf{L_1}$ and $\mathbf{L_2}$ offered the possibility of using these probes for in vivo imaging of cellular thiols (β-/γ-amino alkyl thiols) that are generally abundant in living cells by confocal laser scanning microscopy. To explore this possibility, live HeLa cells were incubated with $\mathbf{L_1}$ or $\mathbf{L_2}$ (20 μM) in

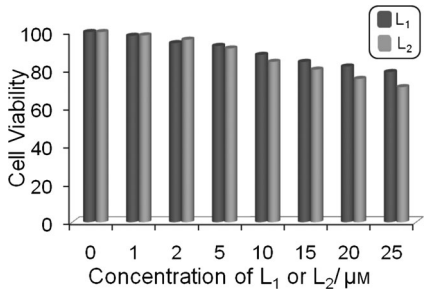

Figure 10. Cell viability values (%) estimated by an MTT proliferation test versus incubation concentration of $\mathbf{L_1}$ (dark grey bars) and $\mathbf{L_2}$ (light grey bars). HeLa cells were cultured in the presence of 0–25 μM of $\mathbf{L_1}$ and $\mathbf{L_2}$ at 37 °C for 12 h (% viability was calculated considering 100 % growth in the absence of $\mathbf{L_1}$ and $\mathbf{L_2}$).

DMSO/aqueous HEPES buffer solution (pH 7.4) for 50 min at 37 °C and then washed thrice with phosphate buffer solution (PBS). The HeLa cells showed no intracellular background fluorescence (Figure 11(B)). After incubation with

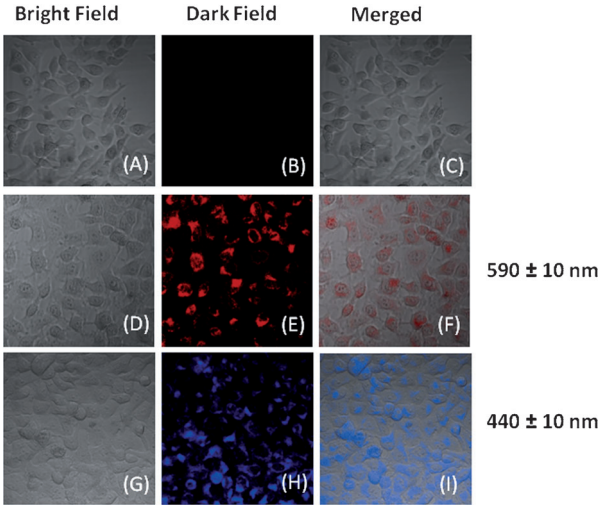

Figure 11. Confocal laser scanning micrographs of living HeLa cells; bright-field transmission image of HeLa cells in the absence of $\mathbf{L_1}$ and $\mathbf{L_2}$ (A); fluorescence image of HeLa cells in the absence of $\mathbf{L_1}$ and $\mathbf{L_2}$ (B), bright-field transmission images of HeLa cells incubated with $\mathbf{L_1}$ (D) and $\mathbf{L_2}$ (G); fluorescence images of HeLa cells incubated with $\mathbf{L_1}$ (from the red channel; E) and $\mathbf{L_2}$ (from the blue channel; H); incubation was performed at 37 °C for 50 min and $[\mathbf{L_1}]$ or $[\mathbf{L_2}] = 20$ μM.

$\mathbf{L_1}$ and $\mathbf{L_2}$, bright-red (590 ± 10 nm) fluorescence images corresponding to $\mathbf{L_1}$-X and intense blue (440 ± 10 nm) fluorescence images corresponding to $\mathbf{L_2}$-X (X = β-/γ-amino alkyl thiols) were observed. Bright-field images of the HeLa cells after incubation with $\mathbf{L_1}$ and $\mathbf{L_2}$ were also acquired (Figure 11(D, G)), and the overlay of confocal fluorescence and bright-field images (Figure 11(F, I)) revealed that fluorescence signals with different intensities were localized in different segments of the HeLa cells, indicating the subcellular distribution of Cys/Hcy. Furthermore, in a control experiment, HeLa cells were pre-treated with 2.0 mM *N*-ethylmaleimide (a thiol blocking agent)[15a,16b,d] for 1 h to reduce the concentration of intracellular thiols prior to incubation with $\mathbf{L_1}$ or $\mathbf{L_2}$ (20 μM) for a further 50 min. A marked fluorescence quenching in the red channel for $\mathbf{L_1}$-X and the blue channel for $\mathbf{L_2}$-X (X = β-/γ-amino alkyl thiols) were observed (Figure S25 in the Supporting Information). Thus, these results revealed that $\mathbf{L_1}$ and $\mathbf{L_2}$ are cell membrane permeable and reacted with intracellular β-/γ-amino alkyl thiols, thereby confirming the utility of these reagents as viable cell imaging reagents for in vivo detection of cellular thiols in living cells.

Detection and analysis of Cys in human blood plasma: Due to the crucial roles that Cys and Hcy play in various physiological processes, the development of an appropriate reagent for quantitative detection/estimation of these biothiols in biological fluids could have enormous significance in biochemistry and clinical chemistry. Knowledge of the concentration of Cys and Hcy in blood plasma is essential for the diagnosis, monitoring, and treatment of homocystinuria and cystathionuria[22] and high Cys in plasma might also contribute to atherosclerosis development in hyperlipidemic patients.[23] Despite this significance, there is as yet no universal technique for the determination of these two important amino acids. The most widely used methods include either direct electrochemical detection after HPLC separation, or pre-/post-column derivatization with monobromobimane (MB)[24]/halogenosulfonylbenzofurazans[25]/*o*-phthalaldehyde (OPA)[26] followed by HPLC separation. Among these methodologies, the post-column technique that is commonly used involves isocratic elution mode and OPA derivatization. The OPA method has the advantages of faster derivatization, not requiring pH adjustment, and isocratic separation. Moreover, the OPA method allows the elution of thiol-containing amino acids as well as other amino acids. This limits the applicability of this method for the selective detection of Cys and/or Hcy in biological fluids without any interference from other amino acids, DNA molecules, and so on. Thus, a great need would be met if an HPLC assay for the selective detection of thiol-containing amino acids such as Cys and Hcy could be developed.[27] Our studies on $\mathbf{L_1}$ and $\mathbf{L_2}$ have revealed that these reagents could be used as selective chemodosimetric probes for the quantitative detection of Cys and Hcy in physiological environments (pH 7.4 and room temperature), and the typical assay time for such detection was approximately 55 min, which is also comparable to those of the limited number of procedures that are known to be followed for this purpose. For quantitative estimation, typical calibration graphs were prepared by plotting I_{598}/I_{528} for $\mathbf{L_1}$ (20 μM) and I_{438}/I_{506} for $\mathbf{L_2}$ (20 μM) with varying [Cys] ($0–120 \times 10^{-5}$ M) after allowing a typical assay time of 55 min. Under the optimal experimental conditions, the typical calibration graphs show good linear fits (Figure 7(A, C)). The concentration level for Cys in healthy plasma typically lies within the range 240–360 μM.[11b] For Hcy, the range is much lower and generally lies between 6 and 12 μM,[28] which is lower than the linear detection limit (Figure 7(B, D)) in our

study. Examples of the quantitative detection of Cys in human plasma have been very rare,[11b–d,17a] and to the best of our knowledge only one previous report describes the quantitative detection of biothiols using a detailed post-column HPLC separation technique.[11d] The feasibility of using $\mathbf{L_1}$ and $\mathbf{L_2}$ for the quantitative estimation of Cys in human plasma was then considered. For this purpose, a modified column-switching HPLC analysis method was developed.

We followed the pre-column HPLC (PTC derivatization) detection methodology based on the SPE technique using an Oasis MCX cartridge and the reagents $\mathbf{L_1}$ and $\mathbf{L_2}$ as chemoselective probes for Cys. Four different sample mixtures for HPLC analysis were prepared: a) 200 μL plasma + 200 μL K_2HPO_4 buffer (pH 6.9); b) 200 μL Cys solution having a concentration of 50 ppm + 200 μL K_2HPO_4 buffer (pH 6.9); c) 200 μL plasma + 200 μL $\mathbf{L_1}$ (2.0×10^{-5} M) + 200 μL K_2HPO_4 buffer (pH 6.9); d) 200 μL plasma + 200 μL $\mathbf{L_2}$ (2.0×10^{-5} M) + 200 μL K_2HPO_4 buffer (pH 6.9). These four sample solutions were passed through the MCX cartridge (see the Supporting Information) to remove macromolecules. After appropriate treatment (see the Supporting Information), PITC was added to each of these four samples (a) to (d). The total Cys and cystine present in the human plasma sample was quantitatively estimated from the integrated area measurement of the desired peak at approximately 11 min for Cys/cystine with reference to the solution of known concentration of Cys (sample (b)) from the HPLC chromatograms of the analyzed samples. Due to the pre-treatment of blood plasma with $\mathbf{L_1}$ or $\mathbf{L_2}$ in samples (c) and (d), respectively, only the Cys present reacted with these molecular probes and formed their corresponding thiazolidine derivatives, as our studies revealed that these molecular probes did not react with cystine (vide supra). HPLC analysis of sample (a) gave the total concentration of Cys + cystine present in the blood plasma for the signal at about 11 min (Figure S24 in the Supporting Information), which was found to be 340 μM. Samples (c) and (d) gave the peak for cystine + PITC (and Cys + PITC, if any remained unreacted during pre-treatment with $\mathbf{L_1}$ or $\mathbf{L_2}$). Comparison of the integrated area of the peaks at about 11 min, obtained for solutions (c) and (d) in HPLC analysis with that of sample (a) gave the relative percentage of Cys that could be detected in the real blood plasma sample. This comparison allowed us to estimate [Cys] in blood plasma as 144.9 μM with $\mathbf{L_1}$ and 133.3 μM with $\mathbf{L_2}$. Figure 12 shows a comparative bar diagram of integrated areas of the peaks at about 11 min for the respective analysed samples (a) to (d). The reductions in the integrated area of the desired peak at about 11 min in the respective chromatograms during the analyses of the samples (c) and (d) clearly indicate that $\mathbf{L_1}$ and $\mathbf{L_2}$ are capable of detecting the Cys present in human blood plasma by thiazolidine formation. Relatively lower values of the estimated [Cys] in blood plasma by using $\mathbf{L_1}$ and $\mathbf{L_2}$ (144.9 μM with $\mathbf{L_1}$ and 133.3 μM with $\mathbf{L_2}$), as compared to that obtained directly from solution (a) (340 μM as total Cys and cystine) presumably reflect the concentration of cystine present in the blood plasma (due to its reaction with PITC in sample (a)). However, one cannot completely rule out the possibility of the presence of a relatively smaller amount of Cys that remained unreacted during the pre-treatment with $\mathbf{L_1}$ (sample (c)) or $\mathbf{L_2}$ (sample (d)). Thus, this result clearly demonstrates the detection ability for Cys in human blood plasma of these two newly synthesized probes $\mathbf{L_1}$ and $\mathbf{L_2}$.

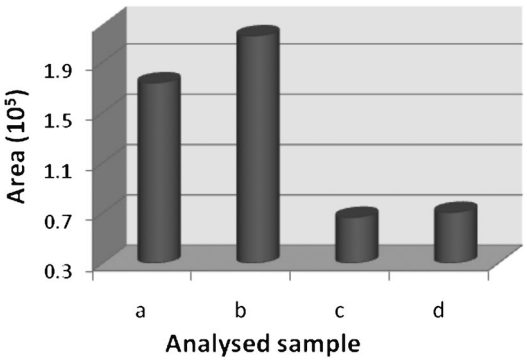

Figure 12. A comparative plot of the integrated areas of different analyzed sample mixtures: a) 200 μL plasma + 200 μL K_2HPO_4 buffer (pH 6.9); b) 200 μL Cys standard solution (50 ppm) + 200 μL K_2HPO_4 buffer (pH 6.9); c) 200 μL plasma + 200 μL $\mathbf{L_1}$ (2.0×10^{-5} M) + 200 μL K_2HPO_4 buffer (pH 6.9); d) 200 μL plasma + 200 μL $\mathbf{L_2}$ (2.0×10^{-5} M) + 200 μL K_2HPO_4 buffer (pH 6.9).

Conclusions

Two different chemodosimetric reagents, $\mathbf{L_1}$ and $\mathbf{L_2}$, have been developed as new ratiometric dual probes (electronic/fluorescent) for the detection of Cys/Hcy. These two new reagents specifically react with Cys/Hcy to afford thiazolidine/thiazinane derivatives with associated visually detectable changes in fluorescence colour. Furthermore, for $\mathbf{L_1}$ changes in solution colour upon thiazolidine/thiazinane formation can also be clearly perceived by the naked eye. DFT studies have confirmed that the thiazolidine or thiazinane formation leads to perturbation of the energies of FMOs as compared to those in $\mathbf{L_1}$ or $\mathbf{L_2}$, thereby accounting for these changes in optical properties. The results of MTT assays have revealed that these probes have low cytotoxicity. Both $\mathbf{L_1}$ and $\mathbf{L_2}$ could be used as in vivo fluorescent imaging reagents for the detection of intracellular distributions of Cys or Hcy. Confocal laser fluorescence scanning microscopic experiments demonstrated that these reagents are cell membrane-permeable and can readily be used to detect the intracellular Hcy/Cys in living HeLa cells. We have also developed a modified version of a column-switching pre-column HPLC method for the quantitative detection of Cys present in human blood plasma using these two reagents ($\mathbf{L_1}$ and $\mathbf{L_2}$). This methodology shows great promise for the detection of amino thiols in human plasma. Importantly, interference from hydroxy amines, different amino acids, cystine, glucose, certain structurally related thiols such as GSH, 2-mercaptoethanol, and CT-DNA is minimal. The remarkable specifici-

ty of these reagents towards Cys/Hcy, coupled with their visually detectable optical recognition, cell membrane permeability, low toxicity, cell imaging application, and the possibility of using them for the detection of Cys in blood plasma by a column-switching HPLC technique, endow them with a certain edge over existing reagents that have been reported for the recognition and detection of these two crucial amino acids under physiological conditions or in blood plasma.

Experimental Section

Materials and methods: 1,2-Diaminoanthracene-9,10-dione, 1,10-phenanthroline, terephthalaldehyde, cysteine, homocysteine, calf thymus DNA, glucose, and 2-mercaptoethanol were obtained from Sigma–Aldrich and were used as received. Other amino acids, glutathione, and all other reagents used in this study were procured from S.D. Fine Chemicals, India. HPLC grade water (Merck, India) was used for all experiments and spectroscopic studies. 1,10-Phenanthroline-5,6-dione (**3**) was synthesized according to a reported literature method.[29]

Materials for HPLC analysis: Amino acid standard mixture, 6 N HCl solution, triethylamine (TEA), disodium hydrogen phosphate (Na_2HPO_4), and standard phenol used for HPLC studies were procured from S.D. Fine Chemicals. Phenyl isothiocyanate (PITC) and HPLC grade sodium acetate trihydrate ($CH_3COONa{\cdot}3H_2O$) were procured from Sigma–Aldrich Chemicals. Blood plasma was collected from the Pharmacology Department of the General Government Hospital at Bhavnagar. HPLC grade acetonitrile (Fisher Scientific) was used, while purified water (Millipore) having a conductance of at least 18 $M\Omega\,cm^{-1}$ was used for the preparation of reagent solutions, eluents, and buffers. All solutions were filtered through a 0.2 μm nylon membrane filter. A Waters Oasis MCX 1 cc/30 mg solid-phase cartridge was used for the extraction of Cys from blood plasma.

Instrumentation: ESI-MS measurements were made on a Waters QToF-Micro instrument. Microanalysis (C, H, N) was performed using a Vario Micro Cube (Elementar) instrument. FTIR spectra were recorded from samples in KBr pellets on a Perkin-Elmer Spectra GX 2000 spectrometer. ^1H and ^{13}C NMR spectra were recorded on Bruker 200 MHz and Bruker Avance-DPX 500 MHz FT NMR spectrometers. Electronic spectra were recorded either using Shimadzu UV-3101 PC or Varian Cary 500 Scan UV/Vis-NIR spectrophotometers. Emission spectra were recorded using a HORIBA JOBIN YVON spectrofluorimeter (Fluorolog). Time-resolved fluorescence measurements were made on an Edinburgh Instruments model OB920 spectrometer using the time-correlated single-photon counting (TCSPC) technique. 360 nm LED and 405 nm laser sources were used as excitation sources. TCSPC data were analysed by iterative convolution of the luminescence decay profiles with the instrument response function using a software package provided by Edinburgh Instruments.

Synthesis of L_1: A solution of terephthalaldehyde (552 mg, 4 mmol) in ethanol (5 mL) was added to a stirred solution of 1,2-diamino-anthraquinone (238.35 mg, 1 mmol) in ethanol (10 mL) in a two-necked round-bottomed flask. A catalytic amount of trifluoroacetic acid (3 drops) was added and the mixture was refluxed for 4 h. Progress of the reaction was monitored by TLC and on completion the mixture was cooled to room temperature. The crude residue was recovered by removal of the solvent under reduced pressure and was further purified by column chromatography on silica gel eluting with $CH_3OH/CHCl_3$ (1:99, *v/v*). The major fraction was collected and the pure product was isolated as a yellow solid after removal of the solvent (yield: 198.34 mg, 56.2%). ^1H NMR (500 MHz, [D_6]DMSO, 25 °C, $SiMe_4$): $\delta = 10.08$ (s, 1H; CHO), 8.573 (d, $J = 8$ Hz, 2H), 8.202 (d, $J = 7$ Hz, 1H), 8.177 (d, $J = 7.5$ Hz, 1H), 8.138 (d, $J = 8.5$ Hz, 1H), 8.078–8.051 (m, 4H), 7.914 ppm (t, $J = 4$ Hz, 2H); ^{13}C NMR (500 MHz, [D_6]DMSO, 25 °C, $SiMe_4$): $\delta = 193.513$, 183.697, 183.082, 137.995, 135.193, 135.063, 134.629, 133.676, 130.419, 130.419, 129.442, 127.501, 126.93, 121.948 ppm; IR (KBr, Nujol): $\tilde{\nu}_{max} = 3299$, 2923, 2854, 2365, 1696, 1665, 1577, 1533, 1485, 1429, 1327, 1293, 1210, 1157, 1007, 841, 713 cm^{-1}; ESI-MS (+ve mode): *m/z* (%): 352.76 (100) [M^+], 384.77 (42) [M+Na^+]; elemental analysis calcd (%) for $C_{22}H_{12}N_2O_3$: C 74.99, H 3.43, N 7.95; found: C 75.3, H 3.45, N 7.92.

Synthesis of L_2: A mixture of terephthalaldehyde (786.6 mg, 5.7 mmol), 1,10-phenanthroline-5,6-dione (400 mg, 1.90 mmol), and ammonium acetate (2.929 g, 38 mmol) in glacial acetic acid (15 mL) was heated at 100 °C for 30 min with stirring. The hot reaction mixture was cooled to room temperature, whereupon a yellow solid separated. The yellow solid was collected by filtration and washed with acetic acid, dilute aqueous $NaHCO_3$ solution, and finally with water. This yellow residue was dried and purified by column chromatography on silica gel eluting with $CH_3OH/CHCl_3$ (5:95, *v/v*) (yield: 390 mg, 63.4%). ^1H NMR (500 MHz, [D_6]DMSO, 25 °C, $SiMe_4$): $\delta = 10.10$ (s, 1H; CHO), 9.065 (d, $J = 3.5$ Hz, 2H), 8.948 (d, $J = 8$ Hz, 2H), 8.478 (d, $J = 8$ Hz, 2H), 8.107 (d, $J = 8$ Hz, 2H), 7.871–7.847 ppm (m, 4H); ^{13}C NMR (500 MHz, [D_6]DMSO, 25 °C, $SiMe_4$): $\delta = 192.457$, 149.136, 147.988, 147.848, 143.690, 143.561, 136.169, 135.00, 130.113, 129.599, 126.438, 123.277 ppm; IR (KBr, Nujol): $\tilde{\nu}_{max} = 3377$, 3075, 2364, 1693, 1606, 1566, 1399, 1212, 1071, 956, 838, 735, 694 cm^{-1}; ESI-MS (+ve mode): *m/z* (%): 347.23 (100) [M+Na^+]; elemental analysis calcd (%) for $C_{20}H_{12}N_4O$: C 74.06, H 3.73, N 17.27; found: C 73.8, H 3.7, N 17.19.

Synthesis of the products of L_1-Cys and L_2-Cys: A solution of cysteine (0.363 g, 3 mmol) in water (5 mL) was added dropwise to a vigorously stirred solution of L_1 (105.6 mg, 0.3 mmol) or L_2 (97.2 mg, 0.3 mmol) in DMSO (20 mL). The reaction mixture was stirred at 70 °C for 6 h and then concentrated to a volume of ~2 mL under vacuum (15 mmHg) at the same temperature. The concentrated mixture was chromatographed on a column of silica gel eluting with CH_3OH/Et_3N (48:2, *v/v*) to give L_1-Cys or L_2-Cys.

L_1-Cys: Yield: 15.2%. ^1H NMR (500 MHz, [D_6]DMSO, 25 °C, $SiMe_4$): $\delta = 13.24$ (s, 1H; COOH), 8.459–8.432 (m, 2H), 8.286–8.199 (m, 3H), 8.144 (m, 2H), 7.98–7.937 (m, 2H), 7.597 (m, 3H), 5.682 ppm (s, 1H; CH_2 methine); IR (KBr, Nujol): $\tilde{\nu}_{max} = 3267$, 3063, 2089, 1661, 1628, 1585, 1483, 1407, 1329, 1191, 1126, 962, 1040, 843, 779, 715 cm^{-1}; ESI-MS (+ve mode): *m/z* (%): 453 (100) [M^+]; elemental analysis calcd (%) for $C_{25}H_{17}N_3O_4S$: C 65.92, H 3.76, N 9.23; found: C 65.69, H 3.8, N 9.18.

L_2-Cys: Yield: 13.8%. ^1H NMR (500 MHz, [D_6]DMSO, 25 °C, $SiMe_4$): $\delta = 13.8$ (s, 1H; COOH), 9.049–9.033 (m, 2H), 8.942 (m, 2H), 8.3 (m, 2H), 7.853–7.846 (m, 2H), 7.631–7.564 (m, 3H), 6.078 ppm (s, 1H; CH_2 methine); IR (KBr, Nujol): $\tilde{\nu}_{max} = 3085$, 2345, 1693, 1606, 1558, 1472, 1399, 1185, 1070, 957, 843, 740, 698 cm^{-1}; ESI-MS (+ve mode): *m/z* (%): 426 (100) [M^+]; elemental analysis calcd (%) for $C_{23}H_{17}N_5O_2S$: C 64.6, H 4.0, N 16.38; found: C 65.42, H 3.94, N 16.2.

General methodology adopted for photophysical studies: Spectrophotometric determinations were made in two different media, specifically or DMSO/aqueous HEPES buffer ((50 mM), pH 7.4, 3:2 (*v/v*)) for receptor L_1 and DMSO/aqueous HEPES buffer ((50 mM), pH 7.4, 8:2 (*v/v*)) for receptor L_2. Samples containing amino acids were typically kept at 37 °C for 18 h before recording UV/Vis and photoluminescence spectra. For luminescence measurements, the excitation wavelengths used were 398 nm (for L_1) and 360 nm (for L_2). The spectral responses of the respective receptors (L_1 or L_2) towards Cys and Hcy were monitored at room temperature. During spectroscopic (absorption and emission) titrations, after each addition of Cys or Hcy the resultant solution was stirred for 30 min before each spectral measurement to ensure complete reaction between L_1 or L_2 (20 μM) and the respective amino acid.

Methodology adopted for HPLC studies: The HPLC method used was based on pre-column derivatization of amino thiols using phenyl isothiocarbamoyl (PITC) as a derivatizing reagent. Reagents L_1 and L_2 were found to react with Cys, present in blood plasma, as was confirmed by this HPLC analysis. Cys and cystine (dimeric amino acid formed by the oxidation of two cysteine residues), present in blood plasma, are inactive in the UV detection that is commonly used for HPLC analysis. Thus, cysteine (Cys) and cystine were first reacted with phenyl isothiocyanate (PITC) to yield UV-active phenylthiocarbamoyl (PTC) moieties that could be analyzed by the UV detector in the HPLC technique. Reaction of PITC with blood plasma gave $[PTC]_{total}$, reflecting the total concentra-

tion of Cys and cystine in the bio-fluid. We have taken advantage of this methodology in establishing the reaction of Cys in blood plasma with the two new reagents ($\mathbf{L_1}$ and $\mathbf{L_2}$), thereby allowing quantitative detection of the Cys present in this bio-fluid. Blood plasma was incubated with either of these two reagents ($\mathbf{L_1}$ or $\mathbf{L_2}$) for 55 min in an appropriate medium to ensure the complete reaction between Cys and $\mathbf{L_1}$ or $\mathbf{L_2}$, and then the mixture was further treated with PITC. Our studies revealed that $\mathbf{L_1}$ and $\mathbf{L_2}$ were unreactive towards cystine, and that PITC reacted with residual cystine present in blood plasma. Thus, PTC formed in this process could be represented as $[PTC]_{cystine}$ and a comparison of this with $[PTC]_{total}$ revealed the amount of Cys that had reacted with the new reagent ($\mathbf{L_1}$ or $\mathbf{L_2}$) and thereby allowed us to quantify the reaction between Cys present in blood plasma and $\mathbf{L_1}$ or $\mathbf{L_2}$.

Responses of $\mathbf{L_1}$ and $\mathbf{L_2}$ to different amino acids, cystine, glucose, CT-DNA, hydroxy/mercapto ethyl amines, and mercaptoethanol: Optical responses of $\mathbf{L_1}$ and $\mathbf{L_2}$ towards different amino acids, specifically Cys, Hcy, glycine (Gly), leucine (Leu), aspartic acid (Asp), proline (Pro), arginine (Arg), lysine (Lys), valine (Val), glutathione (GSH), alanine (Ala), threonine (Thr), histidine (His), tryptophan (Trp), tyrosine (Tyr), serine (Ser), methionine (Met), and cystine, were checked under identical experimental conditions. Responses towards glucose, CT-DNA, hydroxy/mercapto ethylamines, and 2-mercaptoethanol were also screened. In all cases, reactions were carried out either in DMSO/aqueous HEPES buffer (50 mM (pH 7.4), 3:2 (*v*/*v*)) medium for $\mathbf{L_1}$ (20 μM) or in DMSO/aqueous HEPES buffer (50 mM (pH 7.4), 8:2 (*v*/*v*)) medium for $\mathbf{L_2}$ (20 μM), with the different amino acids, cystine, glucose, CT-DNA, ethanolamine, 2-mercaptoethanol, and cysteamine deployed at a concentration of 1.0×10^{-3} M, for 50 min at ambient temperature.

Time-correlated single-photon counting experiments and quantum yield calculations: Time-resolved fluorescence measurements were carried out by the time-correlated single-photon counting (TCSPC) technique using an Edinburgh Instruments model OB920 spectrometer. A 360 nm LED and a 405 nm laser were used as excitation sources. Results of the emission decay traces were analyzed by iterative convolution of the luminescence decay profiles with the instrument response function using a software package provided by Edinburgh Instruments. The relative fluorescence quantum yields (Φ_f) were estimated in DMSO using Equation (1). The integrated emission intensity of quinine sulfate ($\Phi_f=0.54$ in 0.1 M H_2SO_4 at RT)[30] was used as a reference, with a λ_{ext} of 371 nm for $\mathbf{L_1}$ and 365 nm for $\mathbf{L_2}$.

$$\Phi_f = \Phi_f' \, (I_{sample}/I_{std})(A_{std}/A_{sample})(\eta^2{}_{sample}/\eta^2{}_{std}) \quad (1)$$

where Φ_f' is the absolute quantum yield of quinine sulfate, used as reference; I_{sample} and I_{std} are the integrated emission intensities of the sample and the standard, respectively; A_{sample} and A_{std} are the absorbances at the excitation wavelength of the sample and the standard, respectively; and η_{sample} and η_{std} are the respective refractive indices of the sample and standard.

Cell culture and fluorescence imaging: Human cervical cancer cells (HeLa cells) were seeded and grown in Dulbecco's modified Eagle's medium (DMEM) supplemented with 10% foetal bovine serum at 37°C and trypsinized. 1.0×10^4 cells were added to each well in a 24-well culture plate. After growth for 48 h, these cells were incubated with a 20 μM solution of $\mathbf{L_1}$ or $\mathbf{L_2}$ in DMSO/aqueous HEPES buffer (50 mM, pH 7.4) for 60 min at 37°C in the culture medium. After washing thrice with PBS to remove unbound probe molecules, the cells were viewed under a laser scanning confocal microscope (FV1000, Olympus). Furthermore, the cytotoxicities of the respective reagents, $\mathbf{L_1}$ and $\mathbf{L_2}$, towards HeLa cells were determined by conventional MTT assays (see the Supporting Information).[31]

Computational methodology: Geometries were fully optimized at the B3LYP/6-31G(d) level of theory using the Gaussian 03 program.[32] The optimized geometries were checked with imaginary frequencies to identify the ground-state minimum. Single-point calculations were performed at the B3LYP/6-311+G(2d,p) level using the B3LYP/6-31G(d) optimized structures to calculate the energies in each case.

Acknowledgements

A.D. thanks the DST (India) and CSIR (Network project) and S.K.G. thanks the DBT for financial support of this research. P.D., A.K.M., and B.C. acknowledge the CSIR for research fellowships. M.B. acknowledges the UGC for financial support. The authors are grateful to Dr. P. K. Ghosh for his keen interest in this work.

[1] a) T. P. Dalton, H. G. Shertzer, A. Puga, *Annu. Rev. Pharmacol. Toxicol.* **1999**, *39*, 67–101; b) C. K. Mathews, K. E. van Holde, K. G. Ahern, *Biochemistry*, Addison-Wesley, San Francisco, **2000**; c) N. M. Giles, A. B. Watts, G. I. Giles, F. H. Fry, J. A. Littlechild, C. Jacob, *Chem. Biol.* **2003**, *10*, 677–693; d) R. Obeid, W. Herrmann, *FEBS Lett.* **2006**, *580*, 2994–3005.

[2] a) Z. A. Wood, E. Schroeder, J. R. Harris, L. B. Poole, *Trends Biochem. Sci.* **2003**, *28*, 32–40; b) R. Carmel, D. W. Jacobsen, *Homocysteine in Health and Disease*, Cambridge University Press, Cambridge, **2001**; c) E. Camera, M. J. Picardo, *J. Chromatogr. B* **2002**, *781*, 181–206.

[3] M. H. Stipanuk, *Annu. Rev. Nutr.* **2004**, *24*, 539–577.

[4] a) S. Shahrokhian, *Anal. Chem.* **2001**, *73*, 5972–5978; b) K. K. Borowich, M. Swiader, R. Kamiński, H. Kuźniar, Z. Kleinrok, S. J. Czuczwar, *Pol. J. Pharmacol.* **2000**, *52*, 345–352.

[5] a) Review: H. Refsum, P. M. Ueland, O. Nygard, S. E. Vollset, *Annu. Rev. Med.* **1998**, *49*, 31–62; b) S. Seshadri, A. Beiser, J. Selhub, P. F. Jacques, I. H. Rosenberg, R. B. D'Agostino, P. W. F. Wilson, *New Engl. J. Med.* **2002**, *346*, 476–483.

[6] a) R. Clarke, A. D. Smith, K. A. Jobst, H. Refsum, L. Sutton, P. M. Ueland, *Arch. Neurol.* **1998**, *55*, 1449–1455; b) J. L. Mills, J. M. McPartlin, P. N. Kirke, Y. J. Lee, M. R. Conley, D. G. Weir, J. M. Scott, *Lancet* **1995**, *345*, 149–151; c) J. Applebaum, H. Shimon, B. A. Sela, R. H. Belmaker, J. J. Levine, *J. Psychiatr. Res.* **2004**, *38*, 413–416; d) C. van Guldener, C. D. Stehouwer, *Clin. Chem. Lab. Med.* **2003**, *41*, 1412–1417; e) M. M. Villadsen, M. H. Bunger, M. Carstens, L. Stenkjaer, B. L. Langdahl, *Osteoporosis Int.* **2005**, *16*, 411–416; f) D. A. De Luis, N. Fernandez, M. L. Arranz, R. Aller, O. Izaola, E. J. Romero, *J. Diabetes Complications* **2005**, *19*, 42–46.

[7] a) P. Muñiz, P. Sáez, A. Iradi, J. Viña, M. R. Oliva, G. T. Sáez, *Free Radical Biol. Med.* **2001**, *30*, 354–362; b) S. Sengupta, C. Wehbe, A. K. Majors, M. E. Ketterer, P. M. DiBello, D. W. Jacobsen, *J. Biol. Chem.* **2001**, *276*, 46896–46904; c) A. K. Majors, S. Sengupta, B. Willard, M. T. Kinter, R. E. Pyeritz, D. W. Jacobsen, *Arterioscler. Thromb. Vasc. Biol.* **2002**, *22*, 1354–1359; d) P. Yi, S. Melnyk, M. Pogribna, I. P. Pogribny, R. J. Hine, S. J. James, *J. Biol. Chem.* **2000**, *275*, 29318–29323; e) D. Ingrosso, A. Cimmino, A. F. Perna, L. Masella, N. G. De Santo, M. L. De Bonis, M. Vacca, M. D'Esposito, M. D'Urso, P. Galletti, *Lancet* **2003**, *361*, 1693–1699.

[8] a) N. Ercal, P. Yang, N. Aykin, *J. Chromatogr. B* **2001**, *753*, 287–292; b) A. R. Ivanov, I. V. Nazimov, L. Baratova, *J. Chromatogr. A* **2000**, *895*, 157–166; c) G. Chwatko, E. Bald, *Talanta* **2000**, *52*, 509–515; d) Y. V. Tcherkas, A. D. Denisenko, *J. Chromatogr. A* **2001**, *913*, 309–313; e) E. Kaniowska, G. Chwatko, R. Glowacki, P. Kubalczyk, E. J. Bald, *Chromatogr. A* **1998**, *798*, 27–35; f) T. D. Nolin, M. E. McMenamin, J. Himmelfarb, *J. Chromatogr. B* **2007**, *852*, 554–561.

[9] a) P. Ryant, E. Dolezelova, I. Fabrik, J. Baloun, V. Adam, P. Babula, R. Kizek, *Sensors* **2008**, *8*, 3165–3182; b) A. R. Ivanova, I. V. Nazimova, L. A. Baratovab, *J. Chromatogr. A* **2000**, *895*, 167–171; c) G. Chen, L. Zhang, J. Wang, *Talanta* **2004**, *64*, 1018–1023; d) T. Inoue, J. R. Kirchhoff, *Anal. Chem.* **2002**, *74*, 1349–1354.

[10] a) D. Potesil, J. Petrlova, V. Adam, J. Vacek, B. Klejdus, J. Zehnalek, L. Trnkova, L. Havel, R. Kizek, *J. Chromatogr. A* **2005**, *1084*, 134–144; b) N. S. Lawrence, J. Davis, R. G. Compton, *Talanta* **2001**, *53*, 1089–1094; c) N. S. Lawrence, R. P. Deo, J. Wang, *Talanta* **2004**, *63*, 443–449; d) T. Inoue, J. R. Kirchhoff, *Anal. Chem.* **2000**, *72*, 5755–5760; e) S. D. Fei, J. H. Chen, S. Z. Yao, G. H. Deng, D. L. He, Y. F. Kuang, *Anal. Biochem.* **2005**, *339*, 29–35.

[11] a) N. Shao, J. Y. Jin, S. M. Cheung, R. H. Yang, W. H. Chan, T. Mo, *Angew. Chem.* **2006**, *118*, 5066–5070; *Angew. Chem. Int. Ed.* **2006**,

45, 4944–4948; b) O. Rusin, N. N. S. Luce, R. A. Agbaria, J. O. Escobedo, S. Jiang, I. M. Warner, F. B. Dawan, K. Lian, R. M. Strongin, *J. Am. Chem. Soc.* **2004**, *126*, 438–439; c) W. Wang, J. O. Escobedo, C. M. Lawrence, R. M. Strongin, *J. Am. Chem. Soc.* **2004**, *126*, 3400–3401; d) W. Wang, O. Rusin, X. Kim, J. O. Escobedo, O. S. Fakayode, K. A. Fletcher, M. Lowry, C. M. Schowalter, C. M. Lawrence, F. R. Fronczek, I. M. Warner, R. M. Strongin, *J. Am. Chem. Soc.* **2005**, *127*, 15949–15958; e) D. Q. Zhang, M. Zhang, Z. Q. Liu, M. X. Yu, F. Y. Li, T. Yi, C. H. Huang, *Tetrahedron Lett.* **2006**, *47*, 7093–7096.

[12] Y. Sato, T. Iwata, S. Tokutomi, H. Kandori, *J. Am. Chem. Soc.* **2005**, *127*, 1088–1089.

[13] a) F. Tureček, *J. Mass Spectrom.* **2002**, *37*, 1–14; b) K. Marley, D. T. Mooney, G. Clark-Scannell, T. T.-H. Tong, J. Watson, T. M. Hagen, J. F. Stevens, C. S. Maier, *J. Pept. Res.* **2005**, *4*, 1403–1412; c) X. Guan, B. Hoffman, C. Dwivedi, D. P. Matthees, *J. Pharm. Biomed. Anal.* **2003**, *31*, 251–261; d) M. Rafii, R. Elango, G. Courtney-Martin, J. D. House, L. Fisher, P. B. Pencharz, *Anal. Biochem.* **2007**, *371*, 71–81.

[14] a) X. Chen, Y. Zhou, X. Peng, J. Yoon, *Chem. Soc. Rev.* **2010**, *39*, 2120–2135; b) K.-S. Lee, T.-K. Kim, J. H. Lee, H.-J. Kim, J.-I. Hong, *Chem. Commun.* **2008**, 6173–6175; c) B. Zhu, X. Zhang, Y. Li, P. Wang, H. Zhang, X. Zhuang, *Chem. Commun.* **2010**, *46*, 5710–5712; d) H. Li, J. Fan, J. Wang, M. Tian, J. Du, S. Sun, P. Sun, X. Peng, *Chem. Commun.* **2009**, 5904–5906; e) B. Tang, L. Yin, X. Wang, Z. Chen, L. Tong, K. Xu, *Chem. Commun.* **2009**, 5293–5295; f) L. Yi, H. Li, L. Sun, L. Liu, C. Zhang, Z. Xi, *Angew. Chem.* **2009**, *121*, 4094–4097; *Angew. Chem. Int. Ed.* **2009**, *48*, 4034–4037; g) H.-Y. Shiu, H.-C. Chong, Y.-C. Leung, M.-K. Wong, C.-M. Che, *Chem. Eur. J.* **2010**, *16*, 3308–3313; h) B. Tang, Y. Xing, P. Li, N. Zhang, F. Yu, G. Yang, *J. Am. Chem. Soc.* **2007**, *129*, 11666–11667; i) H. S. Jung, K. C. Ko, G.-H. Kim, A.-R. Lee, Y.-C. Na, C. Kang, J. Y. Lee, J. S. Kim, *Org. Lett.* **2011**, *13*, 1498–1501; j) H. S. Jung, J. H. Han, Y. Habata, C. Kang, J. S. Kim, *Chem. Commun.* **2011**, *47*, 5142–5144; k) N. Shao, J. Jin, H. Wang, J. Zheng, R. Yang, W. Chan, Z. Abliz, *J. Am. Chem. Soc.* **2010**, *132*, 725–736; l) X. Chen, S.-K. Ko, M. J. Kim, I. Shin, J. Yoon, *Chem. Commun.* **2010**, *46*, 2751–2753; m) R. N. Dsouza, U. Pischel, W. M. Nau, *Chem. Rev.* **2011**, *111*, 7941–7980; n) Y. Zhou, J. Yoon, *Chem. Soc. Rev.* **2012**, *41*, 52–67.

[15] a) M. Zhang, M. Yu, F. Li, M. Zhu, M. Li, Y. Gao, L. Li, Z. Liu, J. Zhang, D. Zhang, T. Yi, C. Haung, *J. Am. Chem. Soc.* **2007**, *129*, 10322–10323; b) R. Zhang, X. Yu, Z. Ye, G. Wang, W. Zhang, J. Yuan, *Inorg. Chem.* **2010**, *49*, 7898–7903; c) O. Garciá-Beltrán, N. Mena, E. G. Pérez, B. K. Cassels, M. T. Nuñez, F. Wetrlinger, D. Zavala, M. E. Aliga, P. Pavez, *Tetrahedron Lett.* **2011**, *52*, 6606–6609; d) H. L. Chen, Q. Zhao, Y. B. Wu, F. Y. Li, H. Yang, T. Yi, C. H. Huang, *Inorg. Chem.* **2007**, *46*, 11075–11081; e) Z. Yao, H. Bai, C. Li, G. Shi, *Chem. Commun.* **2011**, *47*, 7431–7433.

[16] a) L. Xiong, Q. Zhao, H. Chen, Y. Wu, Z. Dong, Z. Zhou, F. Li, *Inorg. Chem.* **2010**, *49*, 6402–6408; b) L. Xu, Y. Xu, W. Zhu, B. Zeng, C. Yang, B. Wu, X. Qian, *Org. Biomol. Chem.* **2011**, *9*, 8284–8287; c) G.-J. Kim, K. Lee, H. Kwon, H.-J. Kim, *Org. Lett.* **2011**, *13*, 2799–2801; d) X. Cao, W. Lin, Q. Yu, *J. Org. Chem.* **2011**, *76*, 7423–7430; e) J. Bouffard, Y. Kim, T. M. Swager, R. Weissleder, S. A. Hilderbrand, *Org. Lett.* **2008**, *10*, 37–40; f) K. Cui, Z. Chen, Z. Wang, G. Zhang, D. Zhang, *Analyst* **2011**, *136*, 191–195; g) M. Hu, J. Fan, H. Li, K. Song, S. Wang, G. Cheng, X. Peng, *Org. Biomol. Chem.* **2011**, *9*, 980–983; h) Z. Yang, N. Zhao, Y. Sun, F. Miao, Y. Liu, X. Liu, Y. Zhang, W. Ai, G. Song, X. Shen, X. Yu, J. Sun, W.-Y. Wong, *Chem. Commun.* **2012**, *48*, 3442–3444.

[17] a) W. Lin, L. Long, L. Yuan, Z. Cao, B. Chen, W. Tan, *Org. Lett.* **2008**, *10*, 5577–5580; b) X. Zhang, X. Ren, Q.-H. Xu, K. P. Loh, Z.-K. Chen, *Org. Lett.* **2009**, *11*, 1257–1260; c) L. Long, W. Lin, B. Chen, W. Gao, L. Yuan, *Chem. Commun.* **2011**, *47*, 893–895.

[18] T. K. Kim, D. N. Lee, H.-J. Kim, *Tetrahedron Lett.* **2008**, *49*, 4879–4881.

[19] G. Chwatko, H. Jakubowski, *Anal. Biochem.* **2005**, *337*, 271–277.

[20] a) C. Gros, C. Boulegue, N. Galeotti, G. Niel, P. Jouin, *Tetrahedron* **2002**, *58*, 2673–2680; b) C. Gros, N. Galeotti, R. Pascal, P. Jouin, *Tetrahedron* **1999**, *55*, 11833–11842.

[21] F. Tanaka, N. Mase, C. F. Barbas, *Chem. Commun.* **2004**, 1762–1763.

[22] a) S. Yap, E. R. Naughten, B. Wilcken, D. E. Wilcken, G. H. Boers, *Semin. Thromb. Hemostasis* **2000**, *26*, 335–340.

[23] N. Jacob, E. Bruckert, P. Giral, M. J. Foglietti, G. Turpin, *Atherosclerosis* **1999**, *146*, 53–59.

[24] D. W. Jacobsen, V. L. Gatautis, R. Green, *Anal. Biochem.* **1989**, *178*, 208–214.

[25] a) P. E. Cornwell, S. L. Morgan, W. H. Vaughn, *J. Chromatogr. B* **1993**, *617*, 136–139; b) A. Araki, Y. Sako, *J. Chromatogr.* **1987**, *422*, 43–52.

[26] K. Shimada, K. Mitamura, *J. Chromatogr. B* **1994**, *659*, 227–241.

[27] H. Refsum, A. D. Smith, P. M. Ueland, E. Nexo, R. Clarke, J. McPartlin, C. Johnston, F. Engbaek, J. Schneede, C. McPartlin, J. M. Scott, *Clin. Chem.* **2004**, *50*, 3–32.

[28] K. H. Bønaa, I. Njolstad, P. M. Ueland, H. Schirmer, A. Tverdal, T. Steigen, H. Wang, J. E. Nordrehaug, E. Arnesen, K. Rasmussen, *N. Engl. J. Med.* **2006**, *354*, 1578–1588.

[29] J. Bolger, A. Gourdon, E. Ishow, J.-P. Launay, *Inorg. Chem.* **1996**, *35*, 2937–2944.

[30] Reference materials for fluorescence measurement. D. F. Eaton, *Pure Appl. Chem.* **1988**, *60*, 1107–1114.

[31] L. V. Rubinstein, R. H. Shomaker, K. D. Paull, R. M. Simon, S. Tosini, P. Skehan, D. A. Scudiero, A. Monko, M. R. Boyd, *J. Natl. Cancer Inst.* **1990**, *82*, 1113–1117.

[32] Gaussian 03 (Revision E.01), M. J. Frisch, G. W. Trucks, H. B. Schlegel, G. E. Scuseria, M. A. Robb, J. R. Cheeseman, J. A. Montgomery, Jr., T. Vreven, K. N. Kudin, J. C. Burant, J. M. Millam, S. S. Iyengar, J. Tomasi, V. Barone, B. Mennucci, M. Cossi, G. Scalmani, N. Rega, G. A. Petersson, H. Nakatsuji, M. Hada, M. Ehara, K. Toyota, R. Fukuda, J. Hasegawa, M. Ishida, T. Nakajima, Y. Honda, O. Kitao, H. Nakai, M. Klene, X. Li, J. E. Knox, H. P. Hratchian, J. B. Cross, V. Bakken, C. Adamo, J. Jaramillo, R. Gomperts, R. E. Stratmann, O. Yazyev, A. J. Austin, R. Cammi, C. Pomelli, J. W. Ochterski, P. Y. Ayala, K. Morokuma, G. A. Voth, P. Salvador, J. J. Dannenberg, V. G. Zakrzewski, S. Dapprich, A. D. Daniels, M. C. Strain, O. Farkas, D. K. Malick, A. D. Rabuck, K. Raghavachari, J. B. Foresman, J. V. Ortiz, Q. Cui, A. G. Baboul, S. Clifford, J. Cioslowski, B. B. Stefanov, G. Liu, A. Liashenko, P. Piskorz, I. Komaromi, R. L. Martin, D. J. Fox, T. Keith, M. A. Al-Laham, C. Y. Peng, A. Nanayakkara, M. Challacombe, P. M. W. Gill, B. Johnson, W. Chen, M. W. Wong, C. Gonzalez, J. A. Pople, Gaussian, Inc., Wallingford CT, **2004**.

Received: May 9, 2012
Published online: October 11, 2012

